

Entropic effects in the electric double layer of model colloids with size-asymmetric monovalent ions

Guillermo Iván Guerrero-García, Enrique González-Tovar, and Mónica Olvera de la Cruz

Citation: *The Journal of Chemical Physics* **135**, 054701 (2011); doi: 10.1063/1.3622046

View online: <http://dx.doi.org/10.1063/1.3622046>

View Table of Contents: <http://scitation.aip.org/content/aip/journal/jcp/135/5?ver=pdfcov>

Published by the [AIP Publishing](#)

Articles you may be interested in

[Electric double layer for a size-asymmetric electrolyte around a spherical colloid](#)

J. Chem. Phys. **140**, 154703 (2014); 10.1063/1.4871499

[Overcharging and charge reversal in the electrical double layer around the point of zero charge](#)

J. Chem. Phys. **132**, 054903 (2010); 10.1063/1.3294555

[On the effects of ion-wall chemical association on the electric double layer: A density functional approach for the restricted primitive model at a charged wall](#)

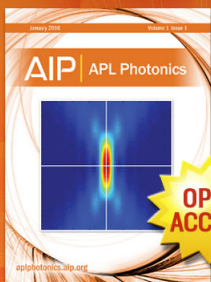
J. Chem. Phys. **125**, 024512 (2006); 10.1063/1.2217943

[X-ray study of the electric double layer at the n-hexane/nanocolloidal silica interface](#)

J. Chem. Phys. **124**, 164704 (2006); 10.1063/1.2189848

[The electrical double layer for a fully asymmetric electrolyte around a spherical colloid: An integral equation study](#)

J. Chem. Phys. **123**, 034703 (2005); 10.1063/1.1949168



Launching in 2016!

The future of applied photonics research is here

OPEN
ACCESS

AIP | APL
Photonics

Entropic effects in the electric double layer of model colloids with size-asymmetric monovalent ions

Guillermo Iván Guerrero-García,¹ Enrique González-Tovar,²
and Mónica Olvera de la Cruz¹

¹*Department of Chemistry and Department of Materials Science and Engineering, Northwestern University, Evanston, Illinois 60208, USA*

²*Instituto de Física, Universidad Autónoma de San Luis Potosí, Álvaro Obregón 64, 78000 San Luis Potosí, San Luis Potosí, México*

(Received 27 May 2011; accepted 14 July 2011; published online 1 August 2011)

The structure of the electric double layer of charged nanoparticles and colloids in monovalent salts is crucial to determine their thermodynamics, solubility, and polyion adsorption. In this work, we explore the double layer structure and the possibility of charge reversal in relation to the size of both counterions and coions. We examine systems with various size-ratios between counterions and coions (ion size asymmetries) as well as different total ion volume fractions. Using Monte Carlo simulations and integral equations of a primitive-model electric double layer, we determine the highest charge neutralization and electrostatic screening near the electrified surface. Specifically, for two binary monovalent electrolytes with the same counterion properties but differing only in the coion's size surrounding a charged nanoparticle, the one with largest coion size is found to have the largest charge neutralization and screening. That is, in size-asymmetric double layers with a given counterion's size the excluded volume of the coions dictates the adsorption of the ionic charge close to the colloidal surface for monovalent salts. Furthermore, we demonstrate that charge reversal can occur at low surface charge densities, given a large enough total ion concentration, for systems of monovalent salts in a wide range of ion size asymmetries. In addition, we find a non-monotonic behavior for the corresponding maximum charge reversal, as a function of the colloidal bare charge. We also find that the reversal effect disappears for binary salts with large-size counterions and small-size coions at high surface charge densities. Lastly, we observe a good agreement between results from both Monte Carlo simulations and the integral equation theory across different colloidal charge densities and 1:1-electrolytes with different ion sizes. © 2011 American Institute of Physics. [doi:10.1063/1.3622046]

I. INTRODUCTION

In recent years, there has been a growth of theoretical and molecular simulations research in which the ionic size asymmetry in colloidal charged model solutions has been taken into account, as an attempt to improve the corresponding description of these relevant coulombic systems. Notably, this inclusion has permitted the elucidation of interesting physical phenomena, such as the existence of a non-zero electrostatic potential for uncharged colloids^{1–4} (without the necessity of considering additional specific interactions), molecular stability mechanisms in RNA,^{5,6} as well as the preferential ionic adsorption in DNA,⁷ ionic channels,⁸ and electrodes.⁹ Recent experiments have also allowed the quantification of the adsorption of ions with different hydration degree at liquid-solid interfaces at molecular level.^{10–12}

One of the first pioneering works dealing with ionic size asymmetry was that of Valleau and Torrie,¹ in which they developed a quasi-point like Poisson-Boltzmann scheme, namely, the modified Gouy-Chapman theory for unequal ionic radii. In that formalism, the ionic size asymmetry is *partially* taken into account by considering different closest approach distances between the ionic species and a charged wall, but otherwise neglecting size correlations between point-ions. Moreover, in that approach it was established that,

for two binary $z : z$ electrolytes, one size-symmetric and the other size-asymmetric, the properties of the electrical double layer are expected to be the same very far from the point of zero charge if the counterions have exactly the same properties in both instances, i.e., for highly charged surfaces the counterions have the leading role, and the specific characteristics of coions are unimportant or completely negligible. This asymptotic behavior was called the dominance of counterions, and is true in the classical Poisson-Boltzmann picture.

On the other hand, in a recent work we have proposed that a size-asymmetric primitive model of ions could be used as a coarse-grained approach to take into account hydration effects coming from a molecular solvent in aqueous solutions.¹³ There, it was shown (theoretically and via molecular simulations) that an effective model with unequal ionic hydration radii displays both an asymmetrical charge neutralization and electrostatic screening of a charged nanoparticle, analogous to the behavior found in a more sophisticated theory in which the solvent molecules (water) are explicitly included.¹⁴ Other interesting consequences of this coarse-grained model are the existence of the phenomenon of surface charge amplification,^{13,15–17} that is, the adsorption of like-charged ions to the first layer adjacent to a weakly charged macroion, or else the appearance of charge reversal (i.e., the overcompensation of the bare colloidal charge by

counterions).^{18–20} Charge reversal due to ion size asymmetry in the context of multivalent salts which induced precipitation was first discussed by Solis and Olvera de la Cruz,²¹ and the conditions for its occurrence in presence of multivalent salts have been recently investigated via molecular simulations.^{22,23}

In the absence of specific short-range interactions, such as van der Waals forces (including ion-dipole and dipole-dipole dispersion forces mediated by a molecular solvent²⁴), the consistent inclusion of ion-ion size correlations is a fundamental ingredient for the occurrence of charge reversal, as it has been pointed out by several authors.^{18,25} In particular, in Ref. 25 it has been shown that, in the restricted primitive model, there is a strong dependence between the appearance of charge reversal (referred in that work as overcharging) regarding the ionic radius and the colloidal charge. Specifically, therein it was proved that, for size-symmetric electrolytes, charge reversal could appear and be enhanced by augmenting either the ionic excluded volume (increasing, for example, the ionic radii at a fixed salt concentration) or by increasing the colloidal surface charge density. Nevertheless, a quantitative relationship between the magnitude of charge reversal and colloidal charge was not established.

Another appealing phenomenon noticed in the restricted primitive model of the electrical double layer is the appearance of anomalous curvatures in the potential vs. charge curves of a spherical macroion surrounded by large monovalent and divalent electrolytes.²⁶ Such peculiar behavior could be relevant in the study of differential capacities of electrified colloidal systems.²⁷ In Ref. 26 the integral equations approach was employed to evidence that the sign of the first derivative of the mean electrostatic potential could be changed by increasing either the ionic radius or the bare colloidal charge in non-dilute size-symmetric electrolytes. A similar behavior has been found recently by density functional theory calculations for the case of a slightly larger macroion,²⁸ and in the planar electrical double layer via Monte Carlo simulations.²⁹

In spite of recent advances in the description of the electrical double layer achieved via mean-field theories,^{30–34} all the phenomenology related in the previous paragraph cannot be predicted by the classical Poisson-Boltzmann theory. In fact, it has also been demonstrated, theoretically and via molecular simulations, that the dominance of counterions is incorrect in the primitive model for large coions.^{19,20} However in such works, only one size asymmetry and one total volume fraction were considered, where the radius of the largest species was twice the radius of the smallest one. Besides, the possibility of having different degrees of effective ionic hydration was not explored. This can be achieved in a coarse-grained model if the ions are allowed to have different size asymmetries and also, for a given size asymmetry, by letting the total ionic volume fractions to vary (via different ionic closest approach distances to the charged surface). Thus, in the present work, we want to study such possible scenarios for a charged spherical macroion as a model system in an extension of the work performed by Messina *et al.*,²⁵ with special emphasis in the influence of the coion size in the electrical double layer (for a fixed counterion size), at the level of the mean electrostatic potential and integrated charge.

II. MODEL, THEORY, AND SIMULATIONS

A rigid, spherical macroion of radius r_M and uniform surface charge density $\sigma_0 = z_M e / 4\pi r_M^2$, immersed in a continuum solvent of dielectric constant ϵ , was considered. The macroion is surrounded by two ionic species, which in the primitive model are treated as hard spheres of radii r_i with embedded point charges, q_i , at their centers. The ionic interaction potential between the macroion and the ionic species is given by

$$U_{ij}(r) = \begin{cases} \infty, & \text{for } r < r_i + r_j, \\ q_i q_j / (4\pi \epsilon_0 \epsilon r), & \text{for } r \geq r_i + r_j, \end{cases} \quad (1)$$

where the subscripts i and j are: $M, -, +$; r is the center-to-center distance between two particles of types i and j , $q_i = z_i e$ is the charge of the species i with valence z_i , e is the protonic charge, and, $q_M = z_M e = 4\pi r_M^2 \sigma_0$ for the spherical macroion. We define the bulk ionic volume fraction as

$$\eta = \frac{4\pi}{3} \sum_{i=-,+} \rho_i r_i^3, \quad (2)$$

such that ρ_i are the bulk ionic densities of anions and cations.

Several theoretical approaches based on the modified Poisson-Boltzmann equations,³⁵ density functional theory,^{36,37} and integral equations^{26,38} have been used to describe the electrical double layer of coulombic systems in spherical geometry. In this work the hypernetted-chain/mean spherical approximation (HNC/MSA) is employed, since in the past it has produced reliable numerical results, in good concordance with molecular simulations. The HNC/MSA approximation for a dispersion of infinitely diluted macroions ($\rho_M = 0$) can be obtained from the Ornstein-Zernike equation, and it is given by¹⁹

$$h_{Mj}(r) = c_{Mj}(r) + \sum_{k=-,+} \rho_k \int h_{Mk}(t) c_{kj}(|\vec{r} - \vec{t}|) dV, \quad (3)$$

for $j = -, +$,

where the $c_{Mj}(r) = -\beta U_{Mj}(r) + h_{Mj}(r) - \ln[h_{Mj}(r) + 1]$ correspond to the HNC closure, and the $c_{kj}(|\vec{r} - \vec{t}|)$ are approximated by the MSA analytical expressions for a bulk electrolyte.^{39,40} Equations (3) constitute a complete set of integral equations that are solved numerically (further details can be consulted elsewhere¹⁹).

Through this work, a charged spherical macroion of radius $r_M = 20$ Å and valence $z_M \geq 0$ immersed in a continuum aqueous medium of dielectric constant and temperature $\epsilon = 78.5$ and $T = 298$ K, respectively, is investigated. This macroion is surrounded by a binary size-asymmetric 1:1, 1 M electrolyte. Several size asymmetries and different bulk ionic volume fractions were analyzed, as detailed in Table I (a graphical representation is depicted in Fig. 1).

The corresponding macroion-ion contact distances are defined for each ionic species as: $d_{M-} = r_M + r_-$ and $d_{M+} = r_M + r_+$.

In size-asymmetric electrolytes, if $r_i < r_j$, the geometric locus defined by a sphere of radius $r_{IHP} = r_M + r_i$ corresponds to the so-called inner Helmholtz plane

TABLE I. Parameters of the monovalent primitive model electrolytes in the Monte Carlo simulations and HNC/MSA calculations. The values of the ionic radii are $r_1 = 1.0625 \text{ \AA}$, $r_2 = 2r_1 = 2.125 \text{ \AA}$, and $r_3 = 4r_1 = 4.25 \text{ \AA}$.

Electrolyte	Anion	Cation	r_-	r_+	η
A1	A	1	r_1	r_1	0.00605
A2	A	2	r_1	r_2	0.02724
A3	A	3	r_1	r_3	0.19670
B1	B	1	r_2	r_1	0.02724
B2	B	2	r_2	r_2	0.04842
B3	B	3	r_2	r_3	0.21788
C1	C	1	r_3	r_1	0.19670
C2	C	2	r_3	r_2	0.21788
C3	C	3	r_3	r_3	0.38734

(IHP), whereas the geometrical location defined by a sphere of radius $r_{OHP} = r_M + r_j$ is known as the outer Helmholtz plane (OHP). In the limiting case when $r_i = r_j$, there is only one Helmholtz plane.

The charge neutralization and electrostatic screening of the colloid can be calculated from the radial distribution functions via the integrated charge,

$$P(r) = z_M + \sum_{i=-,+} \int_0^r z_i \rho_i g_i(r) 4\pi r^2 dr, \quad (4)$$

and the mean electrostatic potential,

$$\psi(r) = \frac{e}{4\pi\epsilon_0\epsilon} \int_r^\infty \frac{P(t)}{t^2} dt. \quad (5)$$

The integrated charge is the net charge (in units of e) enclosed in a sphere of radius r centered in the macroion. This quantity is a measure of charge neutralization of the macroion's bare charge due to the presence of the electrolyte. The mean electrostatic potential evaluated close to the Helmholtz planes is conventionally associated with the well-known zeta potential, ζ ,⁴¹ observed at the slipping plane in electrokinetic phenomena.

Regarding our accompanying simulations, these were performed via a Monte Carlo scheme, by considering a spherical macroion fixed at the center of a cubic box under peri-

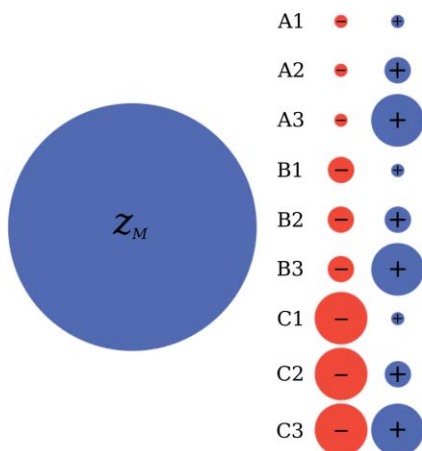


FIG. 1. Schematic representation of the charged spherical colloid and the ionic size asymmetries studied.

odic boundary conditions. The Ewald sums method with conducting boundary-conditions was utilized to take into account correctly the long range behavior of coulombic interactions. The damping constant was $\alpha = 5/L$, where L is the length of the cubic simulation box, and 725 vectors in the k -space were used to compute the reciprocal space contribution to the electrostatic energy. If we denote N_+ and N_- as the number of cations and anions in the simulation box, respectively, the electroneutrality condition imposed in our simulations is given by

$$z_M + N_+ z_+ + N_- z_- = 0. \quad (6)$$

The number of particles employed in each run was around 3500. For the equilibration process 1×10^5 Monte Carlo cycles were performed, and from 4×10^5 (high colloidal charges) up to 1×10^6 (very low colloidal charges) Monte Carlo cycles were used to obtain the canonical average.

III. RESULTS AND DISCUSSION

In order to observe the effect of the coion size in the electrostatic potential close to the macroion's surface, for a given counterion size, in Fig. 2 we display the mean electrostatic potential at the surface, $\psi(r = r_M, \sigma_0)$ (first column), and at the anion's contact-distance, $\psi(r = d_{M-}, \sigma_0)$ (second column), as a function of the surface charge density, σ_0 , for the electrolytes listed in Table I. For positive values of z_M , anions are counterions and cations are coions. Three different counterion sizes are considered, and for a given counterion radius, several asymmetries are studied by varying the coion size. In all cases, it is observed that, for two electrolytes i and j with the same properties of the counterions, to the salt with larger coion corresponds the higher electrostatic screening at the surface and at the counterion's contact distance, that is, $\psi_i(r = r_M, \sigma_0) < \psi_j(r = r_M, \sigma_0)$ and $\psi_i(r = d_{M-}, \sigma_0) < \psi_j(r = d_{M-}, \sigma_0)$, if $\eta_i > \eta_j$. Good agreement is observed between theory and simulations, particularly for low surface colloidal charges.

Another interesting feature found is that, for large counterions (third row), an inverted curvature of the mean electrostatic potential is exhibited independently of the coion size. This kind of inverted curvatures has been reported in the past for electrolytes in the restricted primitive model, where such curvatures were associated with high ionic excluded volume values. Here, we observe not only that high total ionic concentrations are necessary but also that there exists a strong dependency with respect to the counterion size. This is seen clearly when the mean electrostatic potentials at the surface and at the counterion's contact-distance of electrolytes A3 and C1 are compared: both salts have the same, high total ionic excluded volume, but the curvature is inverted only for the electrolyte with the largest counterion size. A similar situation is seen if electrolytes B3 and C2 are collated.

To verify if the behavior of the electrostatic screening observed at the surface and at the counterion's contact-distance, as a function of the coion size for the same counterion size, occurs not only at these geometrical loci but in a whole region

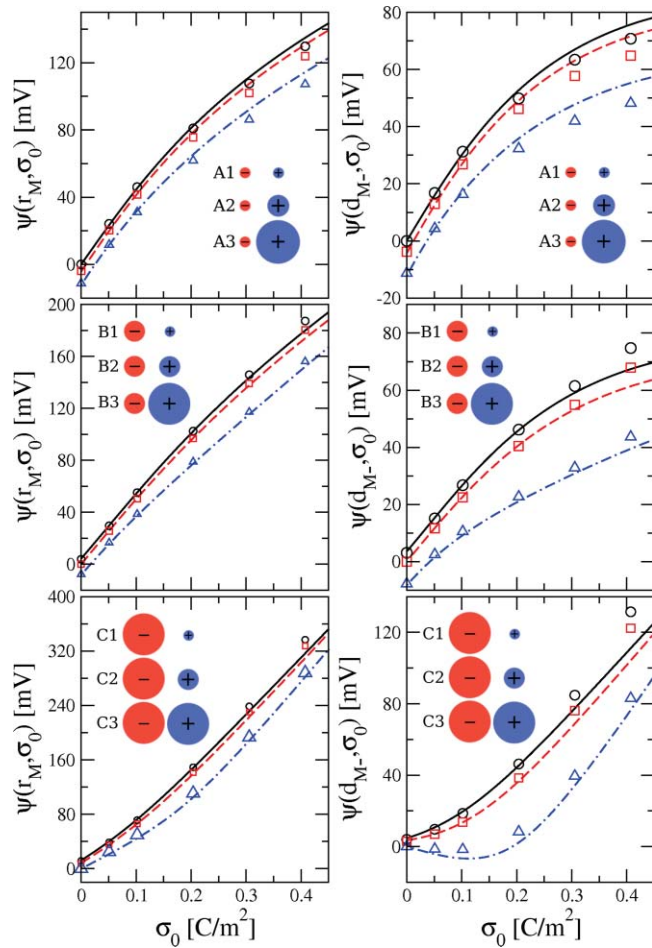


FIG. 2. Mean electrostatic potential at the surface, $\psi(r = r_M, \sigma_0)$ (first column), and at the anion's contact-distance, $\psi(r = d_{M-}, \sigma_0)$ (second column), as a function of the surface charge density σ_0 , for the electrolytes of Table I. The first row corresponds to electrolytes with fixed size anions of type A ($r_- = r_1$), the second row to fixed size anions of type B ($r_- = r_2$), and the third row to fixed size anions of type C ($r_- = r_3$). The solid, dashed, and dotted-dashed lines correspond to HNC/MSA calculations of electrolytes with cation's radius equal to $r_+ = r_1$, $r_+ = r_2$, and $r_+ = r_3$, respectively. The circles, squares, and triangles correspond to MC simulations of electrolytes with cation's radius equal to $r_+ = r_1$, $r_+ = r_2$, and $r_+ = r_3$, respectively.

close to the colloidal surface, we portray in Fig. 3 the $\psi(r)$ for two different colloidal charges: one low ($z_M = 16$, which corresponds to $\sigma_0 = 0.05$ C/m²) and one high ($z_M = 96$, which corresponds to $\sigma_0 = 0.3$ C/m²). There it is observed that $\psi_i(r) < \psi_j(r)$ occurs when $\eta_i > \eta_j$ for r in an interval next to the macroion's surface, which increases along with z_M . It must be noted that in fact, sign inversion in the mean electrostatic potential can appear at low surface charge densities for high ionic excluded volume (see electrolytes A3, B3, C2, and C3). This behavior is also present at high colloidal charges, except for electrolyte C2. In addition, it is observed that, if the coion size is fixed, the mean electrostatic potential is lower for the smaller counterion size very close to the colloidal surface, although can exist regions relatively close to this zone where this situation is reversed (see, for example, either electrolytes B3 and C3 for $z_M = 16$ or electrolytes A3 and B3 for $z_M = 96$ in the first and second row of Fig. 3, respectively). This suggests that experimental measurements of zeta poten-

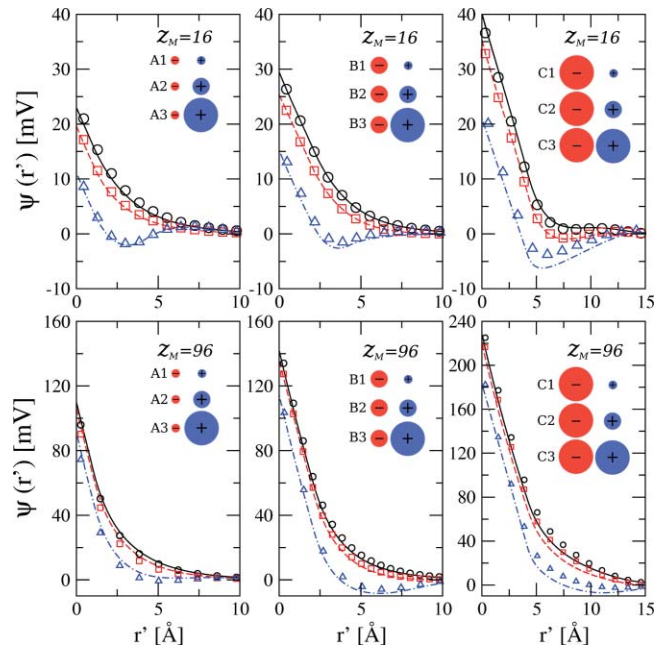


FIG. 3. Mean electrostatic potential, $\psi(r)$, as a function of the distance for a 1:1, 1M electrolyte around a macroion of radius $r_M = 20$ Å and valences $z_M = 16$ (upper row) and $z_M = 96$ (lower row). The first column correspond electrolytes with fixed size anions of type A ($r_- = r_1$), the second column to fixed size anions of type B ($r_- = r_2$), and the third column to fixed size anions of type C ($r_- = r_3$). The solid, dashed, and dotted-dashed lines correspond to HNC/MSA calculations of electrolytes with cation's radius equal to $r_+ = r_1$, $r_+ = r_2$, and $r_+ = r_3$, respectively. The circles, squares, and triangles correspond to MC simulations of electrolytes with cation's radius equal to $r_+ = r_1$, $r_+ = r_2$, and $r_+ = r_3$, respectively. Here, and in the rest of the figures, the distance r' is measured from the surface of the macroion.

tial of charged colloids can indicate opposite trends for the same coion and different counterions in monovalent salts, depending on the position of the shear plane.

The resulting dependence of the electrostatic screening on the size of coions, for the same counterion size, suggests that an analogous behavior at the level of charge neutralization should be expected near the electrified surface. Thus, in Fig. 4 we graph the integrated charge, $P(r)$, associated to the mean electrostatic potentials profiles, $\psi(r)$, previously displayed in Fig. 3. In this figure it is noted that there is a definite region close to the colloidal surface where $P_i(r) < P_j(r)$ if $\eta_i > \eta_j$ for two electrolytes i and j , with the same properties of the counterions but differing in the coion size. *These observations suggest that for a given counterion size, the size of coions rules or dominates the electrostatic screening and charge neutralization of a charged colloid near its surface* (a cartoon is depicted in Fig. 5). The dependence of the ionic adsorption on the ionic excluded volume in this case is analogous to that encountered in a binary size-asymmetric mixture of hard spheres near a colloid: if one of the hard spheres species remain fixed, the increase of the size of the other hard sphere species augments the total adsorption of the hard sphere mixture to a colloidal surface. Moreover, notice that this mechanism is also consistent with the formation of pairs in bulk found in molecular dynamics simulations of size-asymmetric monovalent salts at high concentration, where water is taken into account explicitly.⁴² To illustrate

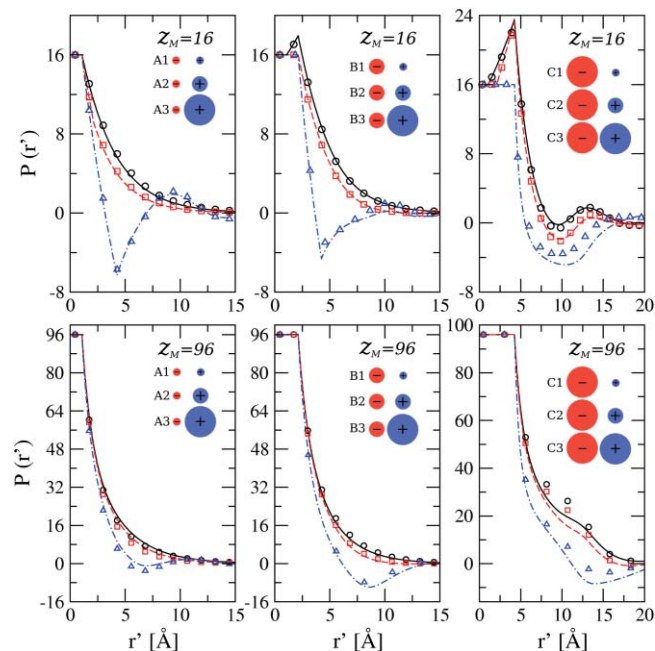


FIG. 4. The same as in Fig. 3 but for the integrated charge, $P(r')$.

this in our model system, let us consider a positively charged macroion immersed in two electrolytes i and j , with anion radii (counterion) $r_{i-} = r_{j-}$ for both salts and varying coion radius (r_{i+} for electrolyte i and r_{j+} for electrolyte j). For concreteness, let us assume that $r_{i+} > r_{j+}$, which implies that $\eta_i > \eta_j$. At high ionic concentrations, the formation of pairs and higher order clusters is more likely for electrolyte j because the ion-ion contact distance between oppositely charged ions is shorter regarding electrolyte i . Thus, for salt i there is a larger total excluded volume and more free counterions than for electrolyte j . Consequently, a higher charge neutralization and electrostatic screening near the colloidal surface of

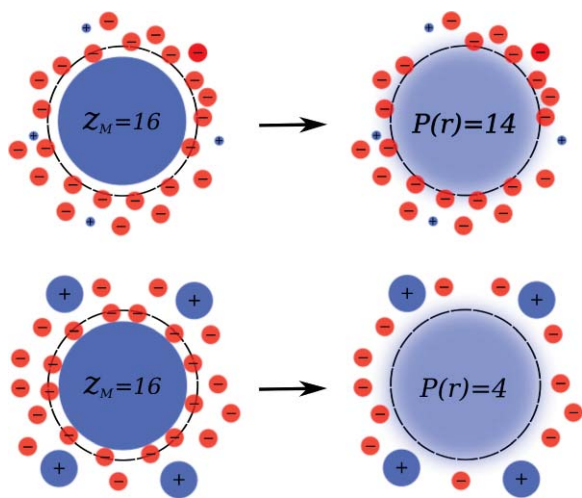


FIG. 5. Cartoon of the ionic cloud of two binary electrolytes with identical properties of the counterion but different coion sizes, around a charged nanoparticle in the primitive model. For the same counterion size, to the salt with larger coion size corresponds the higher charge neutralization (quantified by the integrated charge, $P(r)$) and electrostatic screening close to the electrified colloidal surface. Observe the adjacent counterions in a certain region close to the colloidal surface.

the charged macroion is expected for the former electrolyte, i , than for the latter, j , as it has been shown in Figs. 2, 3, and 4. It is important to point out that, however, formation of ionic clusters in size-asymmetric monovalent salts is significant only at high ionic concentrations; at low electrolyte concentrations this phenomenon becomes negligible because the average interionic distance is very large, which reduces enormously the probability of pairing.⁴²

On the other hand, for electrolytes B1, C1, and C2, the phenomenon of surface charge amplification is manifested; that is, it is observed an increase in the bare colloidal charge of the macroion due to the adsorption of small coions to the first ionic layer adjacent to the macroion's surface. In particular, for very small coions (radius r_1), the increase of counterion size augments significantly the maximum surface charge amplification (compare electrolytes B1 and C1). Surprisingly, this value remained approximately constant for the same large counterion and two different small coions (see electrolytes C1 and C2). Additionally, at low surface charge densities it is seen that if one of the ionic species is large enough, charge reversal (i.e., the overcompensation of the bare colloidal charge by counterions) occurs independently of the ionic sizes. Moreover, given that charge reversal is found at a low surface charge density, this behavior is also expected at higher surface charge densities, in analogy to observations performed in the restricted primitive model for divalent ions, where charge reversal increases monotonically as a function of the colloidal bare charge.⁴³ Charge reversal is observed clearly at high colloidal charges in electrolytes A3, B3, and C3, displaying a shift of the maximum charge reversal position moving away from the macroion, with respect to the low colloidal charge instance. Nevertheless, we find that, for the electrolyte C1, charge reversal is non-existent and, for salt C2, has almost disappeared. In order to study the dependence of charge reversal as a function of the bare colloidal charge, the maximum charge reversal for several size-asymmetric electrolytes and different total ionic volume fractions is plotted in Fig. 6. The maximum charge reversal, Q^* , defined as $Q^* = P(r^*)$ such that $P(r^*) < P(r)$ for all r and positive z_M , is a measure of the overcompensation of the native bare charge by counterions and indicates absence of charge reversal when its value is always zero around a charged colloid. In Fig. 6, we notice that, for large coions and small counterions (electrolytes A3 and B3), a high value of Q^* is seen near the point of zero charge. Moreover, Q^* displays a non-monotonic behavior decreasing in magnitude initially but increasing again as a function of the bare colloidal charge. In addition, it is observed that, for low surface charge densities, the smallest counterions display higher magnitudes of Q^* , although this trend is reversed at higher surface charge densities. A very good agreement is observed between theory and simulations, which deteriorates for high colloidal charges, underestimating (electrolyte A3) and overestimating (electrolyte B3) the magnitude of the maximum charge reversal with respect to the MC results. Also, Fig. 6 shows the effect of increasing the coion radius in Q^* , for large counterions. Near the point of zero charge, charge reversal is observed in both instances; however, the magnitude of Q^* decreases as a function of the colloidal charge. Another interesting feature is that,

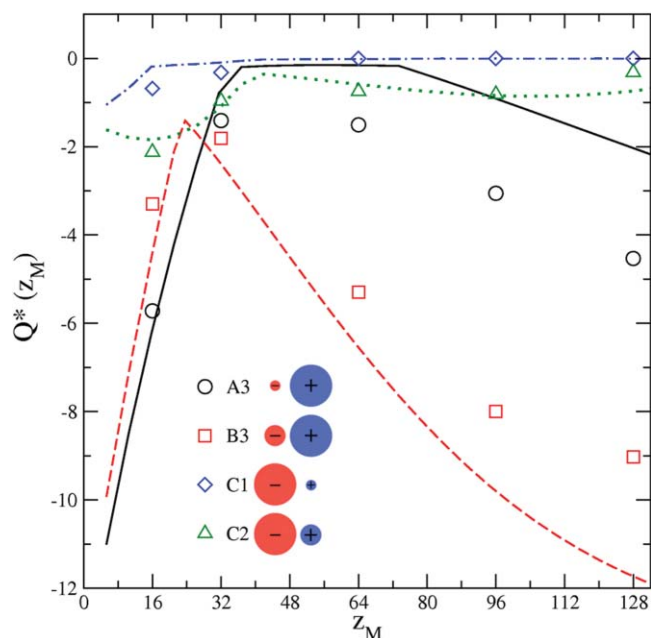


FIG. 6. Maximum charge reversal, Q^* , as a function of the macroion's valence, z_M . Solid, dashed, dotted-dashed, and dotted lines correspond to HNC/MSA calculations for electrolytes A3, B3, C1, and C2, respectively. Circles, squares, diamonds, and triangles correspond to MC simulations for electrolytes A3, B3, C1, and C2, respectively.

for all the range of σ_0 studied, the magnitude of Q^* is higher for the electrolyte with higher total excluded volume. In this case, the agreement between theory and simulations is good for all the σ_0 values.

IV. CONCLUDING REMARKS

The electrical double layer of size-asymmetric monovalent ions around a positive charged macroion in the primitive model has been studied systematically for several ionic size-asymmetries and bulk ionic volume fractions. In particular, for two binary electrolytes, with identical properties of the counterion but different coion sizes, the mean electrostatic potential and integrated charge display a higher charge neutralization and electrostatic screening in a region near the charged surface for that salt with larger coions (i.e., with higher bulk ionic volume fraction). Thus, the main finding of this work is the observation that, *for a given counterion size, the size of coions rules or dominate the charge neutralization and electrostatic screening close to the colloidal surface for size-asymmetric monovalent ions*. We argue that two mechanisms are involved in the above phenomenon: if the counterion's interaction with the macroion is fixed (assuming a surface-ion contact distance d_{M-}), and the excluded volume of counterions remains constant (for a given radius r_-), the augment of the coion size increases the bulk ionic volume fraction (or the total ionic excluded volume) and reduces the formation of pairs and high-order ionic clusters at high salt concentrations, which, in turn, enhances the adsorption of counterions on the macroion's surface. On the contrary, if the coion size decreases, the bulk ionic volume fraction decreases, and there also are less free counterions at high electrolyte concentrations due to the increase of the electro-

static self-attraction between counterions and coions, resulting in a lower electrostatic screening and charge neutralization close to the macroion's surface. Thus, it has been evidenced that, *even in monovalent salts* a rich phenomenology can be found depending on the ionic size and the degree of hydration of each ionic species. In general good agreement has been observed between integral equations theory and simulations.

On the other hand, direct measurements of the integrated charge at molecular level that could corroborate the entropic effects presented above seem to be far from trivial, experimentally speaking. Nevertheless, for diluted charged colloidal particles in presence of a size-asymmetric salt with large counterions, the inversion of the curvature of the electrostatic potential as a function of the surface charge density (see third row of Fig. 2) should be more suitable to be detected in electrophoresis experiments.^{18,44,45}

Finally, some further improvements of the present model could include hydrophobic interactions and image charge correlations. The former seem to play a key role at low electrolyte concentrations, where recent experimental data have shown the possibility of inversion of the electrophoretic mobility in presence of size-asymmetric monovalent ions.⁴⁶ Image charge correlations, on the other hand, have important effects in spherical geometry at low surface charge densities,⁴⁷⁻⁵¹ where notable deviations from analogous systems without polarization effects (that is, considering the same dielectric constant in the whole space) have been observed. Work along this direction is currently underway.

ACKNOWLEDGMENTS

The authors thank William Kung for suggestions on the manuscript. This work was supported by National Science Foundation (NSF) Grant No. DMR-0520513 of the Materials Research Science and Engineering Center program at Northwestern University, and by Consejo Nacional de Ciencia y Tecnología (CONACYT, México), through grant CB-2006-01/58470, and PROMEP.

¹J. P. Valleau and G. M. Torrie, *J. Chem. Phys.* **76**, 4623 (1982).

²M. Valiskó, D. Henderson, and D. Boda, *J. Phys. Chem. B* **108**, 16548 (2004).

³D. Gillespie, M. Valiskó, and D. Boda, *J. Phys.: Condens. Matter* **17**, 6609 (2005).

⁴G. I. Guerrero-García, E. González-Tovar, M. Chávez-Páez, and M. Lozada-Cassou, *J. Chem. Phys.* **132**, 054903 (2010).

⁵D. Lambert, D. Leipply, R. Shiman, and D. E. Draper, *J. Mol. Biol.* **390**, 791 (2009).

⁶A. A. Chen, D. E. Draper, and R. V. Pappu, *J. Mol. Biol.* **390**, 805 (2009).

⁷K. Wang, Y.-X. Yu, G.-H. Gao, and G.-S. Luo, *J. Chem. Phys.* **126**, 135102 (2007).

⁸D. Boda, D. Henderson, and D. D. Busath, *J. Phys. Chem. B* **111**, 11574 (2001).

⁹M. Valiskó, D. Boda, and D. Gillespie, *J. Phys. Chem. C* **111**, 15575 (2007).

¹⁰C. Park, P. A. Fenter, K. L. Nagy, and N. C. Sturchio, *Phys. Rev. Lett.* **97**, 016101 (2006).

¹¹S. S. Lee, P. Fenter, C. Park, N. C. Sturchio, and K. L. Nagy, *Langmuir* **26**, 16647 (2010).

¹²M. Nakamura, N. Sato, N. Hoshi, and O. Sakata, *ChemPhysChem* **12**, 1430 (2011).

¹³G. I. Guerrero-García, E. González-Tovar, and M. Olvera de la Cruz, *Soft Matter* **6**, 2056 (2010).

- ¹⁴P. González-Mozuelos and M. Olvera de la Cruz, *Phys. Rev. E* **79**, 031901 (2009).
- ¹⁵F. Jiménez-Ángeles and M. Lozada-Cassou, *J. Phys. Chem. B* **108**, 7286 (2004).
- ¹⁶Z. Y. Wang and Y. Q. Ma, *J. Chem. Phys.* **133**, 064704 (2010).
- ¹⁷Z. Y. Wang and Y. Q. Ma, *J. Phys. Chem. B* **114**, 13386 (2010).
- ¹⁸M. Quesada-Pérez, E. González-Tovar, A. Martín-Molina, M. Lozada-Cassou, and R. Hidalgo-Álvarez, *ChemPhysChem* **4**, 234 (2003).
- ¹⁹G. I. Guerrero-García, E. González-Tovar, M. Lozada-Cassou, and F. de J. Guevara-Rodríguez, *J. Chem. Phys.* **123**, 034703 (2005).
- ²⁰G. I. Guerrero-García, E. González-Tovar, and M. Chávez-Páez, *Phys. Rev. E* **80**, 021501 (2009).
- ²¹F. J. Solis and M. Olvera de la Cruz, *Eur. Phys. J. E* **4**, 143 (2001).
- ²²A. Diehl and Y. Levin, *J. Chem. Phys.* **129**, 124506 (2008).
- ²³A. Martín-Molina, R. Hidalgo-Álvarez, and M. Quesada-Pérez, *J. Phys.: Condens. Matter* **21**, 424105 (2009).
- ²⁴D. Zhang, P. González-Mozuelos, and M. Olvera de la Cruz, *J. Phys. Chem. C* **114**, 3754 (2010).
- ²⁵R. Messina, E. González-Tovar, M. Lozada-Cassou, and C. Holm, *Europhys. Lett.* **60**, 383 (2002).
- ²⁶E. González-Tovar, F. Jiménez-Ángeles, R. Messina, and M. Lozada-Cassou, *J. Chem. Phys.* **120**, 9782 (2004).
- ²⁷M. B. Partenskii and P. C. Jordan, *Phys. Rev. E* **77**, 061117 (2008).
- ²⁸B. Modak, C. N. Patra, S. K. Ghosh, and J. Vijayasundar, *Mol. Phys.* **109**, 639 (2011).
- ²⁹J. G. Ibarra-Armenta, A. Martín-Molina, and M. Quesada-Pérez, *Phys. Chem. Chem. Phys.* **11**, 309 (2009).
- ³⁰T. E. Colla, Y. Levin, and E. Trizac, *J. Chem. Phys.* **131**, 074115 (2009).
- ³¹T. E. Colla and Y. Levin, *J. Chem. Phys.* **133**, 234105 (2010).
- ³²J. M. Falcón-González and R. Castañeda-Priego, *J. Chem. Phys.* **133**, 216101 (2010).
- ³³J. M. Falcón-González and R. Castañeda-Priego, *Phys. Rev. E* **83**, 041401 (2011).
- ³⁴R. Roa, F. Carrique, and E. Ruiz-Reina, *Phys. Chem. Chem. Phys.* **13**, 3960 (2011).
- ³⁵L. B. Bhuiyan and C. W. Outhwaite, *Condens. Matter Phys.* **8**, 287 (2005).
- ³⁶T. Goel and C. N. Patra, *J. Chem. Phys.* **127**, 034502 (2007).
- ³⁷C. N. Patra, *J. Phys. Chem. B* **114**, 10550 (2010).
- ³⁸H. M. Manzanilla-Granados, F. Jiménez-Ángeles, and M. Lozada-Cassou, *Colloids Surf., A* **376**, 59 (2011).
- ³⁹L. Blum, *Mol. Phys.* **30**, 1529 (1975).
- ⁴⁰K. Hiroike, *Mol. Phys.* **33**, 1195 (1977).
- ⁴¹R. J. Hunter, *Zeta Potential in Colloid Science* (Academic Press, New York, 1981).
- ⁴²A. A. Chen and R. V. Pappu, *J. Phys. Chem. B* **111**, 6469 (2007).
- ⁴³M. Deserno, F. Jiménez-Ángeles, C. Holm, and M. Lozada-Cassou, *J. Phys. Chem. B* **105**, 10983 (2001).
- ⁴⁴M. Quesada-Pérez, E. González-Tovar, A. Martín-Molina, M. Lozada-Cassou, and R. Hidalgo-Álvarez, *Colloids Surf., A* **267**, 24 (2005).
- ⁴⁵C. Schneider, M. Hanisch, B. Wedel, A. Jusu, and M. Ballauff, *J. Colloid Interface Sci.* **358**, 62 (2011).
- ⁴⁶A. Martín-Molina, C. Calero, J. Farudo, M. Quesada-Pérez, A. Travasset, and R. Hidalgo-Álvarez, *Soft Matter* **5**, 1350 (2009).
- ⁴⁷R. Messina, *J. Chem. Phys.* **117**, 11062 (2002).
- ⁴⁸J. Reščič and P. Linse, *J. Chem. Phys.* **129**, 114505 (2008).
- ⁴⁹R. Messina, *J. Phys.: Condens. Matter* **21**, 113102 (2009).
- ⁵⁰Z. Gan and Z. Xu, *Phys. Rev. E* **84**, 016705 (2011).
- ⁵¹A. P. dos Santos, A. Bakhshandeh, and Y. Levin, "Effects of the dielectric discontinuity on the counterion distribution in a colloidal suspension," *J. Chem. Phys.* (in press).